Available online at www.sciencedirect.com
SCIENCE DIRECT®
Physica B 336 (2003) 16–26
PHYSICA B
www.elsevier.com/locate/physb

Surface structure solution by X-ray diffraction: structure completion with positivity and atomicity constraints

D.K. Saldin*, V.L. Shneerson, R. Fung

Department of Physics and Laboratory for Surface Studies, University of Wisconsin-Milwaukee, P.O. Box 413, Milwaukee, WI 53201, USA

Received 21 November 2002; accepted 3 February 2003

Abstract

We propose a method for the solution of surface structures from X-ray diffraction based on the phasing of measured structure factor amplitudes in two stages. First, incorporation of calculated amplitudes and phases of the structure factors of the known underlying bulk structure, together with an iterative algorithm that ensures the positivity of the electron density enables the determination of the amplitudes and phases of the surface structure factors contributing to the crystal truncation rods. Second, inclusion of these structure factors in an iterative algorithm based on Sayre's equations enables the phasing of the superstructure rods.

PACS: 61.10.−i; 61.10.Dp; 68.35.Bs

Keywords: Surface crystallography; X-ray diffraction; Direct method; Phase problem; Surface structure; Crystal truncation rods

1. Introduction

For almost a century, X-ray crystallography has been the workhorse for the determination of the structure of matter at the atomic scale. The bare experimental data from which this information is deduced are a set of measurements of the amplitudes of scattered X-rays. The phases of this scattered radiation are not measured directly, but if they can be deduced, they, together with the measured amplitudes, allow the calculation of the distribution of electrons within a repeat unit of the structure (the unit cell) by a numerical Fourier transform. The determination of the unknown phases is known as the *phase problem* of crystallography.

Crystallographic *direct methods* [1,2] seek to obtain initial estimates of structure-factor phases purely from a knowledge of the measured structure-factor amplitudes, plus general properties of the electron distribution in a unit cell, such as its positivity and atomicity. The adaptation of direct methods to surface crystallography presents a unique set of problems and opportunities. First, although the X-rays are scattered from both the bulk of the crystal and from the surface region, since the bulk structure is usually known, the aim is to recover only the surface structure from the data. In this respect, the task is analogous to that

*Corresponding author.
E-mail address: dksaldin@uwm.edu (D.K. Saldin).

0921-4526/03/$ - see front matter
doi:10.1016/S0921-4526(03)00265-5

of the so-called *structure completion* problem, also addressed in other branches of crystallography [3]. Second, the data consists not of discrete Bragg *spots*, but rather of *rods* of continuous variation of intensity in reciprocal space in a direction perpendicular to the surface [4]. This allows for the possibility of *oversampling* [5] the data relative to the Nyquist frequency [6] in this direction, a feature that aids the recovery of the phases from the data. Third, when the surface is *reconstructed* relative to the bulk, i.e. when its spatial period in a plane parallel to the surface is different (usually greater) than that of the bulk, some of these diffraction rods (the so-called *superstructure rods*, SRs) arise solely from scattering by the surface region of this larger periodicity, while others (the *crystal truncation rods*, CTRs) have *interfering* contributions from both surface and bulk.

It has been suggested [7–10] that the phase problem of crystallography may be addressed by iterative methods that alternatively constrain the solution in real and reciprocal space. The idea was first proposed for electron microscopy by Gerchberg and Saxton [11,12], where the *amplitudes* of complex functions, related by Fourier transforms, are measurable in both real and reciprocal space. The iterative algorithm recovers the phases of the functions in both spaces. An extension of this algorithm when amplitude data is available only in reciprocal space, and where some general constraints may be imposed in real space, such as a spatial localization, or some bounds on the real-space distribution, was subsequently proposed by Fienup and applied to phase determination problems in astronomy and optics [13]. We have earlier proposed an adaptation of this method [9,10] for the problem of *structure completion* in surface X-ray diffraction (SXRD), where initial phases of the CTRs are taken to be those calculated for the known underlying bulk structure. If the data from just the CTRs are used, the resulting solution is known as the *folded* [14] or *average* structure, which consists of the average of that in all bulk unit cell components of the surface unit cell. The *coherent Bragg rod analysis* (COBRA) method of Yacoby et al. [15] employs a different algorithm based on an assumption that the reciprocal-space variation of the complex structure factor of the unknown part of the surface is slower than that of the known bulk. In order to obtain the full structure of the surface unit cell, we had earlier proposed [8–10] resuming the iterations of the same algorithm with the SR data also now included in reciprocal space, but with initial random values for the phases associated with this data, or initial phases interpolated from those of the surface structure factor components of neighboring CTRs. Such an algorithm is based on constraining the diffracted amplitudes to experimentally measured values in reciprocal space, and ensuring the reality and positivity of the electron distribution in real space.

An alternative approach towards a direct method for surface crystallography has been suggested by Rius [16]. This approach seeks to determine the so-called *difference structure*, i.e. the difference between the electron density of the complete surface unit cell and that of the folded structure, from an inverse Fourier transform of phased amplitudes of SRs alone. As such, the difference structure may be positive or negative, although it does satisfy a constraint of *atomicity*, namely that its peaks or dips are substantially localized near the centers of atoms. By exploiting the similarity of the spatial dependence of the difference structure to that of its cube, Rius et al. deduced a *tangent formula* that relates the phase of a structure factor to sums of products of three other structure factors. An iterative algorithm based on these relations has been shown to be capable of phasing the SR amplitudes, and in favorable cases [17] may enable a solution of the surface structure.

In the present paper we point out that, if a structure completion algorithm applied to the CTR data is able to determine the amplitudes and phases of their surface structure factor components (and hence the folded structure), knowledge of these complex structure factors allows a more efficient iterative algorithm, based on the much simpler tangent formula derived from Sayre's equations [18] to determine rapidly the phases of the SR structure factors. Together with the complex surface structure factors from the CTRs, the phased SR structure factors allow a

determination of the complete (unfolded) structure of the surface unit cell.

2. The structure completion problem or holographic analogy

The usual aim of surface crystallography is to recover the unknown surface structure of a sample with a known bulk structure, where both the surface and the bulk contribute to a measured set of diffracted intensities. Thus, the problem of e.g. recovering the surface electron density from SXRD may be regarded as one of structure completion, a problem that has previously been addressed in the field of protein X-ray crystallography [3,19,20].

Suppose that the scattered amplitude from a unit cell of the bulk crystal due to an X-ray photon momentum transfer vector $\mathbf{q}$ is represented by $R_{\mathbf{q}}$, and that of the surface by $O_{\mathbf{q}}$. Then the intensity of the detected X-rays may be written as

$$I_{\mathbf{q}} = |F_{\mathbf{q}}|^2, \tag{1}$$

where the structure factor $F_{\mathbf{q}}$ may be written as the sum:

$$F_{\mathbf{q}} = R_{\mathbf{q}} + O_{\mathbf{q}}. \tag{2}$$

In this expression, $O_{\mathbf{q}} = (F_{\mathbf{q}} - R_{\mathbf{q}})$ is given by a Fourier transform of the electron distribution $\{u_j\}$, i.e.,

$$O_{\mathbf{q}} = \sum_{j=1}^{N} u_j \exp(i\mathbf{q} \cdot \mathbf{r}_j), \tag{3}$$

where $\{u_j\}$ is defined on a uniformly distributed grid of N voxels at positions $\mathbf{r}_j$ within the surface unit cell.

The approach we will use is to determine the amplitudes and phases of the surface structure factors $O_{\mathbf{q}}$ from a knowledge of the measured intensities $I_{\mathbf{q}}$ and calculated values of the amplitudes and phases of the bulk structure factors $R_{\mathbf{q}}$. In a sense, as has been pointed out by Szöke [21], this is quite analogous to the problem of holography [22,23] if the set of intensities $\{I_{\mathbf{q}}\}$ are considered to constitute a *hologram*, the known structure factors $\{R_{\mathbf{q}}\}$ represent a *reference* "wave" and the unknown structure factors $\{O_{\mathbf{q}}\}$ an *object* "wave". Although the numerical methods we use to determine the "object" structure factors have little similarity to the analogue methods of Gabor, nevertheless this is a useful mental analogy, which has also been exploited to solve the problem of structure completion in protein crystallography [19,20]. Once the amplitudes and phases of the set, $\{O_{\mathbf{q}}\}$, of surface structure factors have been determined, it is a straightforward matter to calculate, by means of an inverse Fourier transform, the spatial distribution, $\{u_j\}$, of the electrons in the surface unit cell, and hence to solve the structure.

The problem of surface crystallography has some unique features that are not present in the structure completion problem in the crystallography of bulk samples. This is the presence of the SRs, which are formed solely by diffraction from the unknown surface atoms, and for which there is no contribution from a known part of the structure (or no reference wave, in terms of the holographic analogy).

The strategy we describe in this paper is to use a Fienup-type input–output algorithm, adapted to the present problem of structure completion, to first find both the amplitudes and phases of the surface structure factors contributing to the CTRs, and then to employ an iterative algorithm based on Sayre's relations to find the phases of the SRs (whose amplitudes are accessible by experiment).

3. Phasing of CTRs by an input–output structure completion algorithm

The idea of an input–output feedback loop for phasing that iteratively satisfies conditions in real and reciprocal space has been suggested by Fienup [13] for problems where a non-negative distribution is sought, and where only the amplitudes of the Fourier transform of that quantity are accessible by experiment. The aim is to obtain increasingly better estimates of the phases of this Fourier transform by iteratively satisfying the reciprocal-space constraints and the real-space requirement of the positivity of the sought distribution. Improvement of phase quality is directly correlated with an improved estimate of

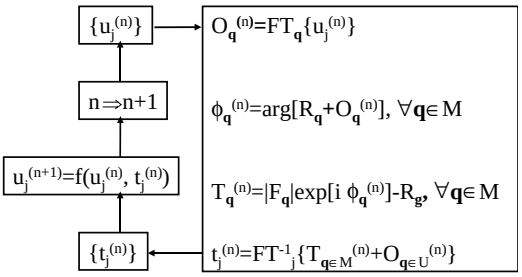

Fig. 1. Flow chart of the input–output feedback loop that converts an input real-space distribution $\{u_j^{(n)}\}$ to an output distribution $\{t_j^{(n)}\}$ by constraining the Fourier transformed quantities to experimental amplitude data. The new input real-space distribution $\{u_j^{(n+1)}\}$ for the next iteration of the feedback loop is calculated from the input and output at the previous iteration by a set of *object domain operations* of the form $u_j^{(n+1)} = f(u_j^{(n)}, t_j^{(n)})$, where f is one of the functions discussed in the text.

that distribution. We show below how a modification of such an algorithm can determine both the amplitudes and phases of the surface structure factors contributing to the CTRs in SXRD [9,10]. A Fourier transform of this subset of surface structure factors would yield an electron distribution representing the folded surface structure referred to above, which has the same lateral periodicity as the underlying bulk structure.

A flow chart for such an algorithm is given in Fig. 1. Starting at the top left-hand corner, suppose $\{u_j^{(n)}\}$ represents the estimate of the folded surface electron density at the nth iteration. Proceeding to the top entry of the right-hand box, we take the Fourier transform ($\mathrm{FT}_{\mathbf{q}}$)

$$O_{\mathbf{q}}^{(n)} = \sum_{j=1}^{N} u_j^{(n)} \exp(\mathrm{i}\mathbf{q}\cdot\mathbf{r}_j), \tag{4}$$

of this distribution by a fast Fourier transform (FFT) algorithm. In X-ray diffraction, the Fourier index $\mathbf{q}$ can be taken to be equal to the difference between the wavevectors of the incident and scattered X-rays. In SXRD, this may be taken as

$$\mathbf{q} = H\mathbf{a}^* + K\mathbf{b}^* + L\mathbf{c}^*, \tag{5}$$

where H, K, and L are Miller indices, $\mathbf{a}^*$ and $\mathbf{b}^*$ are reciprocal lattice vectors parallel to the surface of the bulk lattice, and $\mathbf{c}^*$ the one perpendicular to the surface. The periodicity of the crystal restricts the Miller indices H and K of the CTRs to integer values. If the atomic layers near the surface reconstruct to a lateral unit cell greater than that of the bulk, the X-rays may scatter also into SRs,which may be characterized by fractional values of H and/or K. In the case of the CTRs, the breaking of the periodicity perpendicular to the surface due to the crystal truncation and, in the case of the SRs, the finite thickness of the surface slab, allows scattering into directions corresponding to a continuous variation of L [8]. In the following we describe an application of this algorithm solely to the CTR data.

The dimensions of the parallelepiped reciprocal-space array of $\{O_{\mathbf{q}}^{(n)}\}$ (and consequently the real-space grid spacing of $\{u_j^{(n)}\}$) are chosen so that all the values of the wavevector difference $\mathbf{q}$ belonging to the set $\mathscr{M}$ of measured structure factors $|F_{\mathbf{g}}|$ may be embedded within it. The set of elements in the same parallelepiped reciprocal-space array not belonging to $\mathscr{M}$ may be termed the unmeasured set $\mathscr{U}$.

The next step is the evaluation of the arguments of the Fourier coefficients $R_{\mathbf{q}} + O_{\mathbf{q}}^{(n)}$ for all $\mathbf{q}\in\mathscr{M}$ and the assignment of their arguments to the phases

$$\phi_{\mathbf{q}}^{(n)} = \begin{cases} \arg[R_{\mathbf{q}}] & \text{if } n = 0, \\ \arg[R_{\mathbf{q}} + O_{\mathbf{q}}^{(n)}] & \text{if } n > 0 \end{cases} \tag{6}$$

for all $\mathbf{q}\in\mathscr{M}$. The "target" Fourier coefficients $T_{\mathbf{q}}^{(n)}$ are then computed by the formula

$$T_{\mathbf{q}}^{(n)} = |F_{\mathbf{q}}| \exp[\phi_{\mathbf{q}}^{(n)}] - R_{\mathbf{q}} \quad \forall\mathbf{q}\in\mathscr{M}. \tag{7}$$

The inverse Fourier transform

$$t_j^{(n)} = \frac{1}{N}\sum_{\mathbf{q}} [T_{\mathbf{q}\in\mathscr{M}}^{(n)} + O_{\mathbf{q}\in\mathscr{U}}^{(n)}] \exp(-\mathrm{i}\mathbf{q}\cdot\mathbf{r}_j), \tag{8}$$

at the last step within the right-hand box gives rise to the output electron distribution, $\{t_j^{(n)}\}$.

Thus, in such an input–output scheme [13], the box on the right of the flow chart transforms an *input* electron distribution $\{u_j^{(n)}\}$ to an *output* one $\{t_j^{(n)}\}$ at iteration n by combining experimental information about the measured amplitudes $|F_{\mathbf{q}}|$ with the current estimates of the phases $\phi_{\mathbf{q}}^{(n)}$ associated with those amplitudes. The boxes on

the left of the flow chart describe the steps in the transformation of the input, $\{u_j^{(n)}\}$, and output, $\{t_j^{(n)}\}$, at the nth iteration to the input $\{u_j^{(n+1)}\}$ at the next iteration. These steps are known as the *object-domain operations*, and may be written in the general form $u_j^{(n+1)} = f(u_j^{(n)}, t_j^{(n)})$. Fienup [13] suggested four specific prescriptions for such operations. In the present paper we use only the simplest of these, which Fienup termed an *error-reduction* algorithm, since he was able to prove that it always converged towards a solution that simultaneously satisfied the constraints in real and reciprocal space. The real-space operations of the error-reduction algorithm are

$$u_j^{(n+1)} = \begin{cases} t_j^{(n)} & \text{if } t_j^{(n)} > 0, \\ 0 & \text{otherwise.} \end{cases} \tag{9}$$

The progress of successive estimates of the relevant Fourier coefficients of a particular reciprocal space scattering vector $\mathbf{q} \in \mathscr{M}$ belonging to a CTR may be visualized from Fig. 2. The distance from the center of the circle to its perimeter represents the magnitude $|F_\mathbf{q}|$ of the measured structure factor of the entire sample (bulk plus surface). $R_\mathbf{q}$ is a fixed vector in this amplitude-phase diagram, representing the bulk structure factor that is known in both amplitude and phase. The surface contribution to the total structure factor must join the end of the vector $R_\mathbf{q}$ to the circle perimeter. The problem is that since the phase of this vector is initially unknown, there are an infinite number of such possible vectors. The first (unweighted difference Fourier [3]) estimate, $T_\mathbf{q}^{(0)}$, of this surface structure factor takes this phase to be equal to that $R_\mathbf{q}$ of the bulk. $T_\mathbf{q}^{(0)}$ is thus taken to be parallel to $R_\mathbf{q}$, as shown in Fig. 2.

The inverse Fourier transform of the surface structure factors $\{T_\mathbf{q}^{(0)}\}$ produces the initial output real-space distribution $\{t_j^{(0)}\}$. After an application of the object-domain operations to produce the new input distribution $\{u_j^{(n)}\}$ $(n > 0)$, the Fourier transform of the latter gives the surface structure factor estimates $\{O_\mathbf{q}^{(n)}\}$. The phase $\phi_\mathbf{q}^{(n)}$ is defined by the vector sum of $R_\mathbf{q}$ and $O_\mathbf{q}^{(n)}$ as shown in the figure. Since, in general, the magnitude of this vector sum will not be equal to $|F_\mathbf{q}|$, this vector is extended (or contracted) without change in direction until it touches the circle perimeter. The vector joining the end of the bulk structure factor $R_\mathbf{q}$ and that point on the circle's perimeter is now defined as the new estimate $T_\mathbf{q}^{(n)}$.

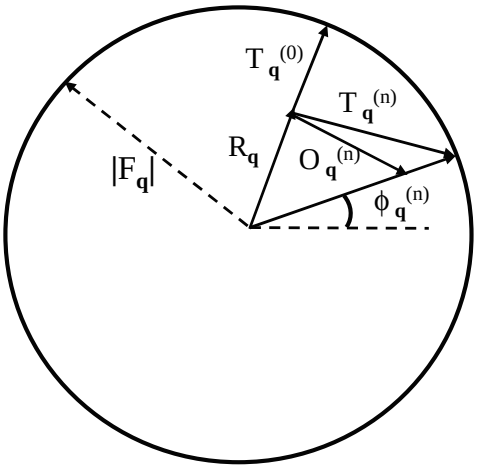

Fig. 2. Amplitude-phase diagram indicating the relationships amongst the various component structure factors of scattering vector $\mathbf{q}$. The circle has a radius of $|F_\mathbf{q}|$, the measured amplitude of Bragg reflection $\mathbf{q}$. $R_\mathbf{q}$ represents the structure factor of the known bulk unit cell. This is known in both amplitude (length) and phase (angular separation from the dashed line). The (unweighted) difference Fourier estimate of the structure factor of the unknown part of the structure (the surface) is represented by the vector $T_\mathbf{q}^{(0)}$, which has the same phase (direction) as $R_\mathbf{q}$. $O_\mathbf{q}^{(n)}$ is the estimate of the same structure factor at the nth iteration $(n > 0)$ of the input–output feedback loop, formed from the input distribution $\{u_j^{(n)}\}$ of the surface electron density. Since the end of the vector sum of $R_\mathbf{q}$ and $O_\mathbf{q}^{(n)}$ will not in general lie on the circumference of the circle, the length of this vector is adjusted to the circle radius. The target structure factor $T_\mathbf{q}^{(n)}$ of the surface is then constructed such that when added vectorially to $R_\mathbf{q}$ it is equal in both amplitude $|F_\mathbf{q}|$ and phase $(\phi_\mathbf{q}^{(n)})$ to the new estimate $F_\mathbf{q}^{(n)}$ of the structure factor of the entire structure (bulk and surface). The Fourier transform of the target structure factors $\{T_\mathbf{q}^{(n)}\}$ forms the output distribution $\{t_j^{(n)}\}$ at the nth iteration. The object domain operations then construct a new input distribution $\{u_j^{(n+1)}\}$ and the process repeated until $O_\mathbf{q}^{(n+1)}$ and $T_\mathbf{q}^{(n+1)}$ (or $\{u_j^{(n+1)}\}$ and $\{u_j^{(n)}\}$) converge.

After several iterations, as convergence is approached, $O_\mathbf{q}^{(n)}$ and $T_\mathbf{q}^{(n)}$ $\forall \mathbf{q} \in \mathscr{M}$ tend to merge. The resulting phase $\phi_\mathbf{q}^{(n)}$ of $R_\mathbf{q} + O_\mathbf{q}$ (or of $R_\mathbf{q} + T_\mathbf{q}$) is the final estimate of the phase of the measured structure factor $F_\mathbf{q}$. When supplemented by the Fourier coefficients $O_\mathbf{q}^{(n)}$ $\forall \mathbf{q} \in \mathscr{U}$, the inverse

Fourier transform of the combined set gives the final estimate of the folded surface electron distribution as that to which both $\{t_j^{(n)}\}$ and $\{u_j^{(n)}\}$ eventually converge.

It should be noted that, due to the continuous distribution of SXRD intensities along a diffraction rod, this data may be *oversampled* in reciprocal space relative to the Nyquist frequency corresponding to the thickness of the slab representing a surface unit cell. In general, the Fourier transform of such oversampled data would be expected to generate non-zero electron densities in a real-space slab of greater thickness than the physical surface slab. The efficiency of the phasing process is further enhanced by setting the electron densities to zero *at each iteration* in the part of this notional slab that is not expected to contain surface atoms [5].

In order to recover the full electron distribution of a surface unit cell of larger lateral dimensions than that of the bulk unit cell, it is necessary also to include the structure factors of the SRs. Since the SRs do not have contributions from the underlying bulk, the amplitudes of their surface structure factors are directly measurable from experiment. However, for the same reason, the bulk structure factors are of no use in suggesting even initial estimates for the phases of the SR structure factors. Nevertheless, as we demonstrate in the following, knowledge of the amplitudes and phases of the CTRs allows the rapid determination of the unknown phases of the SRs by an iterative algorithm based on Sayre's equations [18], that assume both atomicity and positivity of the electron distribution.

4. Phasing of the SRs from phased CTRs and Sayre's equations

In Section 2 we expressed the Fourier coefficients $O_{\mathbf{q}}$ as Fourier transforms of surface electron distribution (Eq. (3)). An alternative expression in terms of the form factor f_s of the sth atom of the surface unit cell is

$$O_{\mathbf{q}} = \sum_s f_s(\mathbf{q}) \exp(i\mathbf{q} \cdot \mathbf{r}_s). \tag{10}$$

Since the majority of electrons are localized near the centers of their respective atoms s, we see that Eq. (10) will be consistent with Eq. (3) if

$$f_s(\mathbf{q}) = \sum_{j \in (\text{atom } s)} u_j \exp[i\mathbf{q} \cdot (\mathbf{r}_j - \mathbf{r}_s)] \tag{11}$$

and the summation over j is here performed over just the electrons in the voxels associated with atom s. That is, an atomic form factor may be regarded as a Fourier transform with an origin defined at the center of the atom, of the electrons of that atom. To put it another way, expressing the surface structure factor in the form (10) is equivalent to an assumption that the sought electron distribution consists of a sum of separable distributions associated with each atom.

Now consider the structure factor of the same surface unit cell due to the square of this electron distribution. It may be written as

$$G_{\mathbf{q}} = \sum_s g_s(\mathbf{q}) \exp(i\mathbf{q} \cdot \mathbf{r}_s), \tag{12}$$

where

$$g_s(\mathbf{q}) = \sum_{j \in (\text{atom } s)} u_j^2 \exp[i\mathbf{q} \cdot (\mathbf{r}_j - \mathbf{r}_s)]. \tag{13}$$

If all the atoms are assumed equal (the *equal-atom* approximation) we may write

$$\frac{f_s(\mathbf{q})}{g_s(\mathbf{q})} = \theta_{\mathbf{q}}, \tag{14}$$

a quantity independent of the atom index s. Hence, from Eqs. (10) and (12)

$$O_{\mathbf{q}} = \theta_{\mathbf{q}} G_{\mathbf{q}}. \tag{15}$$

By substituting Eq. (13) into Eq. (12) we find

$$G_{\mathbf{q}} = \sum_{j=1}^{N} u_j^2 \exp(i\mathbf{q} \cdot \mathbf{r}_j). \tag{16}$$

Comparing this with Eq. (3), and applying the convolution theorem, we obtain

$$G_{\mathbf{q}} = \sum_{\mathbf{q}'} O_{\mathbf{q}'} O_{\mathbf{q}-\mathbf{q}'} \tag{17}$$

and, using Eq. (15),

$$O_{\mathbf{q}} = \theta_{\mathbf{q}} \sum_{\mathbf{q}'} O_{\mathbf{q}'} O_{\mathbf{q}-\mathbf{q}'}. \tag{18}$$

This is Sayre's celebrated relation [18] amongst structure factors. The quantity $\theta_{\mathbf{q}}$ may be calculated from a knowledge of the atomic charge distribution (in the case of unequal atoms, this may be taken as the average atomic charge distribution). However, if, as commonly the case with an unknown surface structure, these atomic charge distributions are unknown, a more useful relationship (sometimes known as a tangent formula) that follows from Eq. (18) since $\theta_{\mathbf{q}}$ is real, is

$$\arg[O_{\mathbf{q}}] = \arg\left[\sum_{\mathbf{q}'} O_{\mathbf{q}'} O_{\mathbf{q}-\mathbf{q}'}\right]. \tag{19}$$

We can establish phases of the surface structure factors giving rise to the superstructure rods by rewriting this as the recursion relation:

$$\arg[O_{\mathbf{q}}^{(n+1)}] = \arg\left[\sum_{\mathbf{q}'} O_{\mathbf{q}'}^{(n)} O_{\mathbf{q}-\mathbf{q}'}^{(n)}\right], \tag{20}$$

where n is an iteration index. The H and K Miller indices of the scattering vector $\mathbf{q}$ are taken to correspond to those of the SRs. Each of the surface structure factors in each term on the RHS corresponds to data from either a CTR or an SR. Both the amplitudes and phases of the surface structure factors contributing to a CTR are kept fixed throughout the iterations at the final values found from the output of the Fienup algorithm for the CTRs described earlier. The amplitudes of the SR structure factors are kept fixed at their values deduced directly from experimental measurements of the SR intensities, but since their phases are initially unknown, they are assigned random values at the outset (corresponding to iteration $n = 0$ on the RHS).

A first pass through the algorithm for all values of $\mathbf{q}$ corresponding to the SRs overwrites these random phases with those calculated via Eq. (20). Incrementing n by 1, and substituting these updated SR surface structure factors on the RHS allows a new estimate of the SR phases via Eq. (20). The values to which these phases converge after several iterations are our final assignment of the phases of the surface structure factors of the SRs. Finally, the distribution of electrons in the surface unit cell is calculated by the inverse Fourier transform

$$u_j = \frac{1}{N} \sum_{\mathbf{q}} O_{\mathbf{q}} \exp(-\mathrm{i}\mathbf{q} \cdot \mathbf{r}_j). \tag{21}$$

5. Test calculation

We have tested this idea by attempting to recover a surface structure from simulated SXRD data. The example we chose was a hypothetical structure of $c(2 \times 2)\mathrm{K}/\mathrm{TiO_2}(0\,0\,1)$. The unit cell of bulk TiO_2 (rutile) in a (0 0 1) direction consists of mutually orthogonal unit vectors of magnitudes $a = 4.59$ Å, $b = 2.96$ Å and $c = 4.59$ Å. The **a** and **b** unit vectors lie in a plane parallel to the surface (the basal plane), while **c** is perpendicular to it. The structure consists of a sequence of Ti-O-O-Ti-O-O layers parallel to the basal plane. The two sequences of Ti-O-O layers are related to one another by mirror reflection across a b–c plane. We assume that the outermost bulk layer is the last of the above-named O planes.

We assume that the lowest surface layer is at a height of $0.1c$(= 0.46 Å) above that expected of the next Ti layer of a bulk structure, but that it has a $c(2 \times 2)$ periodicity relative to the bulk structure parallel to the surface. Referring atom positions relative to a three-dimensional (2×2) unit cell on top of the outermost bulk unit cell, with an origin in a plane half way between the outermost O layer of the bulk and the expected position of Ti atoms in an unrelaxed structure, and whose height is the same as that of a bulk unit cell ($c = 4.59$ Å), the surface atoms were assumed to be at the following positions:

Ti: (0.0, 0.0, 0.2), (0.5, 0.5, 0.2)
K: (0.3, 0.0, 0.2), (0.8, 0.5, 0.2)
K: (0.15, 0.5, 0.54), (0.65, 0.0, 0.54)

where all coordinates are expressed as fractions of $2a$, $2b$ and c, respectively. It should be emphasized that, as yet, the true structure of this surface has not been determined from experimental data, and so the above model is an arbitrary one chosen purely for this test. A plan view of this structure is shown in Fig. 3(a), where for clarity the bulk atoms are not shown. Two orthogonal projections

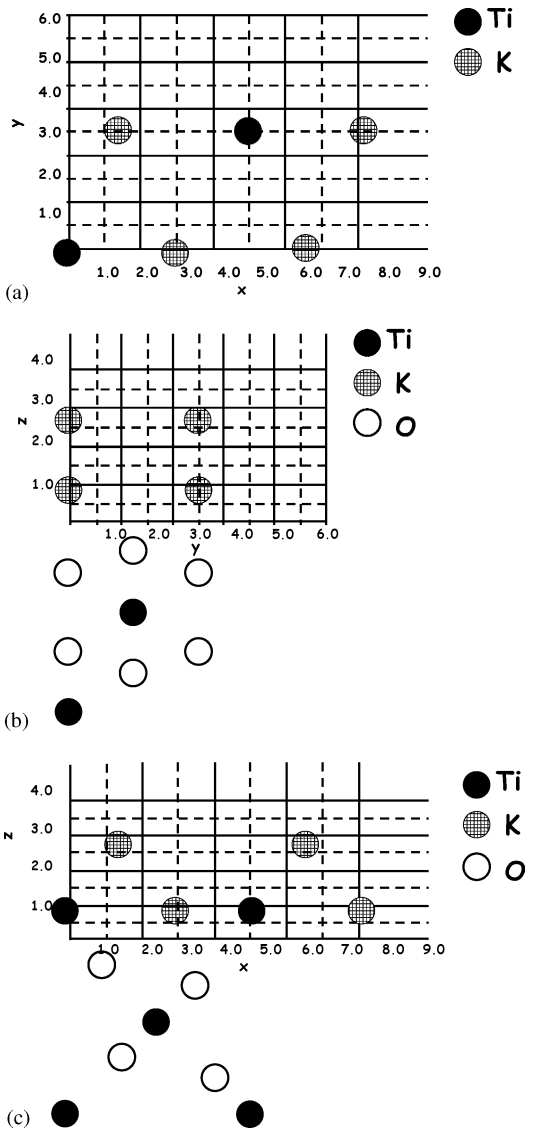

Fig. 3. Three orthogonal projections of the model of the $c(2\times 2)K/TiO_2(0\,0\,1)$ surface assumed in the calculations. (a) Plan view, projected onto a plane parallel to the surface. Only the atoms in the surface unit cell are shown. (b) side view, projected onto a plane defined by the *b*- and *c*-axis (c) side view, projected onto a plane defined by the *a*- and *c*-axis. Shown in (b) and (c) are all atoms of a (2×2) surface unit cell as well as those of an underlying (1×1) bulk unit cell. The chemical species of the atom symbols are indicated on the upper right of each panel.

viewed from directions parallel to the unit vectors **a** and **b** of the basal plane are shown in Figs. 3(b) and 3(c), respectively.

Test "experimental" data were calculated for this structure by a standard SXRD program. Relative to a (2×2) surface unit cell, this test data consists of a set of SXRD intensities corresponding to scattering vectors **q** with integer values of the Miller index pairs (H,K), each varying from -7 to 8 in integer intervals, and a few values of the third Miller index, $L=0.2,0.4,$ and 0.6. The centered (2×2) surface unit cell restricts the combination of H and K Miller indices to those of even values of $(H+K)$ (see the diffraction pattern of Fig. 4, which marks the projections of the CTRs and SRs onto a plane parallel to the surface). Furthermore, due to the mirror planes perpendicular to the surface and parallel to the H-axis, it is necessary only to know

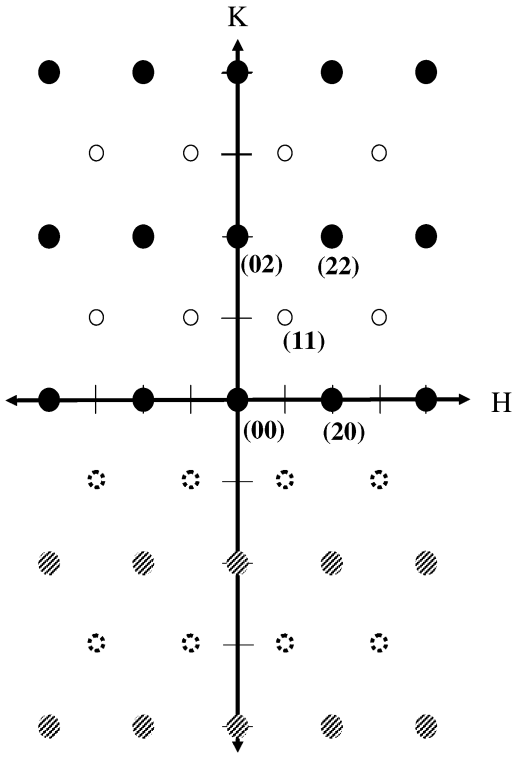

Fig. 4. Cut through reciprocal space parallel to the surface, intersecting the crystal truncation rods (CTRs) and SRs from a $c(2\times 2)K/TiO_2(0\,0\,1)$ surface. There is a mirror plane of symmetry perpendicular to the paper and passing through the H-axis. Only the intersected rods corresponding to $K\geqslant 0$ are symmetrically inequivalent. The filled circles represent the intersections of CTRs and the open circles the SRs.

values of intensities of the rods with positive values of K. The combination of mirror symmetry and Friedel's Law allows the deduction of the intensities of all other diffraction rods of Fig. 4 for both positive and negative values of L. The additional data required of our algorithm are, of course, calculated values of the amplitudes and phases of the corresponding structure factors of the underlying truncated bulk structure of $TiO_2(0\,0\,1)$. These were also calculated by the same computer program. Due to the fact that the bulk unit cell is half the size of the surface unit cell in the directions of the a- and b-axis, the bulk lattice contributes only to the CTRs, which are the subset of rods with even values of the Miller indices H and K.

The CTR data formed the input to the error-reduction form of the Fienup algorithm of Section 3. This determines the amplitudes and phases of the surface contributions to the CTRs. In our present example, convergence was achieved after about 25 iterations. An inverse Fourier transform of this set of structure factors gives the *folded* version of the electron distribution of the surface unit cell, which has the same periodicity parallel to the surface as the bulk structure. An inverse Fourier transform of just the so-called "in-plane" surface structure factors, corresponding to low values of L gives the *projection* of this electron distribution onto a plane parallel to the surface. In practice, measurements of "in-plane" data are quite common. They correspond to measurements of scattered X-rays at glancing take-off angles to the surface from the glancing incidence of incoming X-rays. Of course, due to the fact that both source and detector have to lie outside the plane of the surface, inevitably there has to be a surface-normal component of $\mathbf{q}$. However, the value of L can be kept down to approximately 0.1 or 0.2. This is usually small enough that the set of such surface structure factors may be treated as the Fourier components of a *projection* of the surface electron distribution onto a plane parallel to the surface. The *folded* structure *projected* onto a plane parallel to the surface, calculated from $L = 0.2$ data by the Fienup algorithm from this simulated data is shown as a contour map in Fig. 5 (we choose the $L = 0.2$ data since they are generally experimentally measurable, yet of a low enough L value that their Fourier transform with respect to Miller indices H and K is practically indistinguishable from those of $L = 0$).

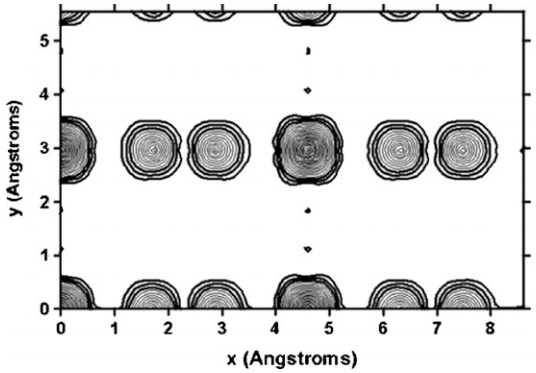

Fig. 5. Contour map, calculated from the Fourier transform of the surface structure factors of Miller index $L = 0.2$ contributing to the CTRs of the $c(2 \times 2)K/TiO_2(0\,0\,1)$ surface. The structure factors were found from the input–output phasing algorithm described in the text by incorporating calculated structure factors from the known underlying bulk crystal. To a good approximation, this represents the surface electron density *projected* onto a plane parallel to the surface and *folded* into a unit cell of the underlying bulk unit cell. There are 25 equally-spaced contour levels from 0 to the maximum value.

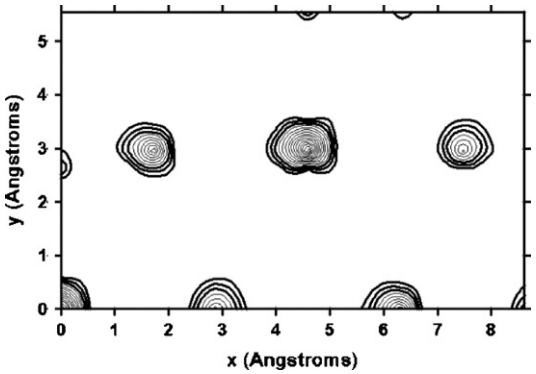

Fig. 6. Contour map, calculated from the Fourier transform of the surface structure factors of Miller index $L = 0.2$ of both the CTRs and also the SRs of the $c(2 \times 2)K/TiO_2(0\,0\,1)$ surface. The latter structure factors are calculated from the former by the iterative algorithm also described in the text, based on Sayre's equations. To a good approximation, this represents the electron density of the surface unit cell *projected* onto a plane parallel to the surface. There are 15 equally-spaced contour levels from 0 to the maximum value.

We then proceeded to attempt to recover the true projected electron distribution of a (2×2)

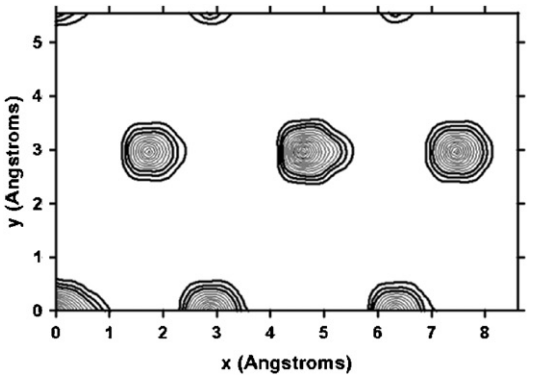

Fig. 7. Contour map of the electron density of the surface unit cell *projected* onto a plane parallel to the surface. This is calculated from the model of the $c(2\times 2)K/TiO_2(0\,0\,1)$ surface assumed in our calculations. There are 16 equally-spaced contour levels from 0 to the maximum value. Note the excellent agreement with the contour map of Fig. 6.

unit cell by using the recursion relation (20) to phase the "in-plane" SR structure factors. In this case, convergence of the algorithm (20) occurred after about 10 iterations. The inclusion of both the CTR- and SR-phased "in-plane" data in the inverse Fourier transform (21) resulted in the projected electron distribution shown in Fig. 6. Comparison of this distribution with that from structure factors calculated from the atomic model of the surface used for our test (Fig. 7), and with the projection (Fig. 3) of the atomic model assumed in our calculations, shows remarkable agreement of the main features.

6. Conclusions

We have described a procedure for determining the distribution of electrons in a surface unit cell from experimental measurements of the intensities of crystal truncation and superstructure rods (CTRs and SRs) in surface X-ray diffraction (SXRD).

The solution requires first the isolation and retrieval of the amplitudes and phases of the surface structure factors contributing to the CTRs. This is done by first recognizing and calculating the contributions to these CTRs from the generally known structure of the underlying bulk. An algorithm that incorporates this knowledge, and successively constrains the solution to the measured amplitudes of the CTRs in reciprocal space and restricts the real-space electron distribution to be non-negative is used to determine the complex surface structure factor components of the CTRs, and hence the folded surface structure. Unlike the method proposed by Yacoby et al. [15] for determining this folded structure, we make no assumptions about the relative rates of variation of the surface and bulk structure factors.

Our next step is to use an iterative algorithm based on the tangent formula from Sayre's equations to determine the phases of the SRs from this knowledge of the amplitudes and phases of the CTR surface structure factors determined at the earlier step. The combination of the complex structure factors contributing to the CTRs and SRs enables the determination of the complete surface structure, unlike the method of Rius et al. [16], which phases only the SRs, and is thus only able to determine the difference between the unfolded and folded structures. Also, since the Sayre tangent formula relates the phases of structure factors to sums of products of pairs (rather than the triplets of the formula of Rius et al.) of other structure factors, the algorithm is much simpler and more computationally tractable, and leads to a rapid solution in a small number of iterations.

Acknowledgements

We acknowledge stimulating discussions with Wolfgang Moritz and Jordi Rius. R.F. is grateful for financial support in the form of a UWM Graduate School Fellowship. Support for this work was also provided by the US National Science Foundation (Grant No.: DMR-9815092) and the US Department of Energy (Grant Nos.: DE-FG02-01ER45926 and DE-FG02-84ER45076).

References

[1] C. Giacovazzo, Direct Methods in Crystallography, Academic Press, London, 1980.

[2] M.M. Woolfson, Direct Methods in Crystallography, Oxford University Press, Oxford, 1961.
[3] W. Cochran, Acta Crystallogr. 4 (1951) 408.
[4] I.K. Robinson, D.J. Sweet, Rep. Prog. Phys. 55 (1992) 599.
[5] L.D. Marks, Phys. Rev. B 60 (1999) 2771.
[6] See e.g. W.H. Press, S.A. Teukolsky, W.T. Vetterling, B.P. Flannery, Numerical Recipes in Fortran 90, Cambridge University Press, Cambridge, 1996.
[7] L.D. Marks, W. Sinkler, E. Landree, Acta Crystallogr. A 55 (1999) 601.
[8] D.K. Saldin, R.J. Harder, H. Vogler, W. Moritz, I.K. Robinson, Comput. Phys. Commun. 137 (2001) 12.
[9] D.K. Saldin, R.J. Harder, V.L. Shneerson, W. Moritz, J. Phys.: Condens. Matter 13 (2001) 10689.
[10] D.K. Saldin, R.J. Harder, V.L. Shneerson, W. Moritz, J. Phys.: Condens. Matter 14 (2002) 4087.
[11] R.W. Gerchberg, W.O. Saxton, Optik 35 (1972) 237.
[12] R.W. Gerchberg, Opt. Acta 21 (1974) 709.
[13] J.R. Fienup, Opt. Lett. 3 (1978) 27.
[14] M. Sowwan, Y. Yacoby, J. Pitney, R. MacHarrie, M. Hong, J. Cross, D.A. Walko, R. Clarke, R. Pindak, E.A. Stern, Phys. Rev. B 66 (2002) 205311.
[15] Y. Yacoby, R. Pindak, R. MacHarrie, L. Pfeiffer, L. Berman, R. Clarke, J. Phys.: Condens. Matter 12 (2000) 3929.
[16] J. Rius, C. Miravitlles, R. Allmann, Acta Crystallogr. A 52 (1996) 634.
[17] X. Torrelles, J. Rius, F. Boscherini, S. Heun, B.H. Mueller, S. Ferrer, J. Alvarez, C. Miravitlles, Phys. Rev. B 57 (1998) R4281.
[18] D. Sayre, Acta Crystallogr. 5 (1952) 60.
[19] A. Szöke, Acta Crystallogr. A 49 (1993) 853.
[20] V.L. Shneerson, D.L. Wild, D.K. Saldin, Acta Crystallogr. A 57 (2001) 163.
[21] A. Szöke, Phys. Rev. B 47 (1993) 14044.
[22] D. Gabor, Nature 161 (1948) 777.
[23] R.J. Collier, C.B. Burckhardt, L.H. Lin, Optical Holography, Academic Press, San Diego, 1971.